POLITECNICO DI TORINO
Repository ISTITUZIONALE

Unlocking Versatile and Non-Volatile Bandwidth Tunability in Silicon Photonic Contra-Directional-Coupler-Based Filter Devices

Original
Unlocking Versatile and Non-Volatile Bandwidth Tunability in Silicon Photonic Contra-Directional-Coupler-Based Filter Devices / Tunesi, L., Amin Mahdian, M., Shafiee, A., Curri, V., Carena, A., Bardella, P., Nikdast, M.. - ELETTRONICO. - (2024), pp. 702-705. (ECOC 2024; 50th European Conference on Optical Communication Frankfurt (Ger) 22-26 September 2024).

Availability:
This version is available at: 11583/3015104 since: 2026-09-08T14:16:00Z

Publisher:
IEEE

Published
DOI:

Terms of use:

This article is made available under terms and conditions as specified in the corresponding bibliographic description in the repository

Publisher copyright
IEEE postprint/Author's Accepted Manuscript

©2024 IEEE. Personal use of this material is permitted. Permission from IEEE must be obtained for all other uses, in any current or future media, including reprinting/republishing this material for advertising or promotional purposes, creating new collecting works, for resale or lists, or reuse of any copyrighted component of this work in other works.

(Article begins on next page)

09 October 2026

Unlocking Versatile and Non-Volatile Bandwidth Tunability in Silicon Photonic Contra-Directional-Coupler-Based Filter Devices

Lorenzo Tunesi [(1*)], Mohammad Amin Mahdian[(2)], Amin Shafiee[(2)], Vittorio Curri[(1)], Andrea Carena[(1)], Paolo Bardella[(1*)], and Mahdi Nikdast[(2*)]

[(1)] Department of Electronics and Telecommunications, Politecnico di Torino, Turin, Italy
[(2)] Department of Electrical and Computer Engineering, Colorado State University, Fort Collins, CO, USA
Contact: {paolo.bardella,lorenzo.tunesi}@polito.it,{mahdi.nikdast,amin.mahdian}@colostate.edu

Abstract *We present a novel bandwidth control mechanism using phase-change materials (Sb_2Se_3) to enable wide-bandwidth tunability in silicon photonic grating-assisted contra-directional couplers. The bandwidth dynamic range, obtained using experimentally validated simulation models, is 9.1 nm, surpassing the 3.2 nm achievable with conventional thermal control methods.* ©2024 The Author(s)

Introduction

Silicon photonic (SiPh) Grating-Assisted Contra-Directional Couplers (GACDCs) are versatile integrated photonic components, allowing for a broad range of add-drop filtering and switching applications[1],[2]. They are characterized by a wide-band flat-top spectral response and a flexible design space that allows precise tailoring to the desired application. Additionally, grating waveguide geometry can be customized for more exotic applications outside traditional single-mode/polarization filtering, such as mode multiplexing and polarization splitting/rotation, further enhancing their importance as potential building blocks within photonic integrated circuits[3],[4].

Despite their numerous promising attributes, GACDCs suffer from drawbacks such as their large footprint, particularly when narrow filtering or dynamic bandwidth control are required[5],[6]. Their active tunability is also critical, as these devices depend on conventional Thermo-Optic (T-O) or Electro-optic (E-O) tuning mechanisms, which have some limitations within the SiPh platform. Dynamic bandwidth control requires modulation of the effective index along the propagation direction and is therefore limited by the maximum achievable index shift. As a result, these mechanisms are better suited for minor adjustments or calibration, rather than major shifts in the bandwidth. Moreover, they require continuous static power consumption to preserve the index change.

We propose a novel bandwidth control mechanism for GACDCs leveraging SiPh-compatible Phase-Change Materials (PCM), which are a class of materials whose crystalline/amorphous fraction can be dynamically controlled, thus allowing for modulation of their optical properties[7]. The index contrast between the crystalline and amorphous states in PCMs can realize a larger dynamic control than traditional T-O/E-O-based methods while providing a nonvolatile solution to maintain the state. After exploring several PCMs with different layer geometries, we opted to design and analyze a Sb_2Se_3-based GACDC and evaluate its performance in the C-band, resulting in enhanced non-volatile tuning capabilities compared to a thermally controlled device. The accuracy of our simulation models and the passive design of the devices considered have been validated through experimental measurements of multiple fabricated GACDCs.

Device Design and PCM Analysis

GACDCs are four-port devices that implement wavelength-selective add-drop filtering using Bragg's grating structures in an otherwise uncoupled asymmetric waveguide system. The distributed Bragg mirror allows for the frequency-selective coupling of the forward propagating mode of the input waveguide to the backward mode of the second[8]. By precisely engineering the width and pitch (Λ) of the grating, the contra-directional coupling coefficient can be tailored for a specific wavelength. The target channel from the input waveguide is therefore reflected and coupled into a second waveguide, while the remaining spectrum propagates through. This behavior is symmetrically mirrored on the add port, leading to an add-drop filtering operation.

Fig. 1(a) depicts the main geometrical parameters of a GACDC, which define the spectral response. The drop channel central wavelength depends on the phase-match condition, defined by the average effective index of the coupled waveguide system and the pitch of the grating, while the bandwidth depends primarily on the corrugation geometry and the coupling gap. Beyond the choice of optimal waveguide geometry, different design strategies can enhance the performance. Undesired intra-waveguide reflections can be minimized by shifting the corrugations by 180° between the two sides of the waveguide[9]. Side lobes and out-of-band ripples can be attenuated by introducing grating apodization, which smooths the transition between intrinsic waveguides and corrugated regions, e.g., using the hyperbolic tangent-based profile:

$$\Delta w\,(n) = \frac{\Delta w_{\max}}{2}\left[1+\tanh\left(\beta\left(1-2\left|\frac{2n-N}{N}\right|^{\alpha}\right)\right)\right],$$

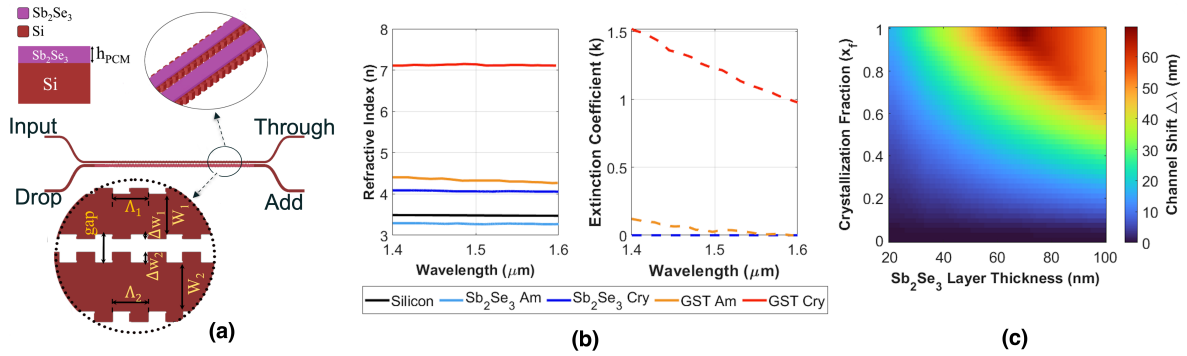

Fig. 1: (a) Schematic of the GACDC structure under investigation. (b) Refractive index and extinction coefficient for Sb_2Se_3 and $Ge_2Sb_2Te_5$. (c) Drop channel wavelength shift ($\Delta\lambda$) as a function of the crystallization fraction (X_f) and Sb_2Se_3 thickness.

where α=3,β=2, and n is the index of the period.

In this article, the devices (based on T-O and PCM control) have been designed and simulated considering all aforementioned design optimizations. Considering Fig. 1(a), in our GACDCs, W_1 = 570 nm and W_2 = 430 nm. The coupling gap is 200 nm, and Δw_1 and Δw_2 are 60 nm and 100 nm, respectively. Both structures use a symmetric grating period ($\Lambda_{1,2}$ = 318 nm for the T-O device and $\Lambda_{1,2}$ = 297 nm for the PCM-based structure) to achieve the same central drop wavelength despite the difference in waveguide geometry due to the added Sb_2Se_3 layer. This is done to allow for a direct comparison in the same reference bandwidth. The length of both devices is n=2000 periods.

GACDC structures are traditionally tuned via T-O effects, by adjusting the effective indices of the waveguides using segmented metallic heaters to calibrate the central wavelength and tailor the bandwidth[10],[11]. However, T-O-based tuning is limited by silicon T-O properties as well as thermal crosstalk, which affects adjacent components. Moreover, the volatile nature of T-O tuning makes it an energy-inefficient solution. On the other hand, PCMs offer a novel solution for controlling device properties, enabling extensive tuning of SiPh waveguide characteristics. PCMs exhibit a large shift in optical properties between their amorphous and crystalline states while remaining stable in the intermediate states. This allows for modulation of optical properties as a function of the crystallization fraction (X_f), which can be done thermally or optically[12],[13].

By depositing a PCM layer on top of silicon waveguides, we can leverage the shift in the refractive index to control the spectral properties of our device. The maximum index shift, as well as the absorption profile, can vary wildly between different PCMs (see Fig. 1(b)), leading to different choices of material depending on the application requirements. We have explored two PCMs as candidates for dynamic bandwidth control, namely $Ge_2Sb_2Te_5$ (GST) and Sb_2Se_3. The optical and thermal properties have been extracted from[14], and the data have been used to fit the materials in our device simulations. GST-enhanced structures have been proposed in static switching applications[15]. However, GST imposes significant losses as a result of its high extinction coefficient in the crystalline state. Meanwhile, the shift in channel wavelength is relatively smaller when Sb_2Se_3 is used due to its smaller refractive index contrast compared to GST. This enables a finer control over the phase-match condition, hence the drop response bandwidth. Moreover, Sb_2Se_3 has negligible absorption in the C-band (1.53 µm–1.56 µm), making it an excellent candidate for phase-only modulation needed in our proposed application.

The challenge of achieving precise small-step crystallization ratios can be mitigated by choosing the most suitable material and the optimal PCM layer geometry. The geometry of the Sb_2Se_3 layer is determined by analyzing the drop-channel wavelength shifts based on the crystalline fraction (X_f) and the thickness of the PCM layer (h_{PCM}), as shown in Fig. 1(c). By selecting h_{PCM}=50 nm, the phase-match condition can be tuned across the entire C-band ($\Delta\lambda \approx$45 nm). Further increase in the PCM layer thickness would not be beneficial for a C-band tunable add-drop filter, only leading to higher modal mismatch between the PCM-loaded waveguide in the GACDC and the default silicon waveguides, as well as necessitating a more precise control mechanism.

Simulation Models and Bandwidth Tunability

The devices (based on T-O and PCM control) have been simulated using different techniques and models, ranging from the Eigen Mode Expansion (EME) method and 3D Finite-Difference Time-Domain (FDTD) method available in ANSYS Lumerical[16], to Coupled-Mode Theory (CMT) analytical models[17] that we developed in MATLAB. These models were further refined and verified using experimental results from the fabrication of passive GACDCs, fabricated using electron-beam lithography at Applied Nanotools (Fig. 2(a)–(b)).

The response of our fabricated device shows a $\Delta\lambda \approx$30 nm blue shift, attributed to manufacturing variations such as reduced corrugation width

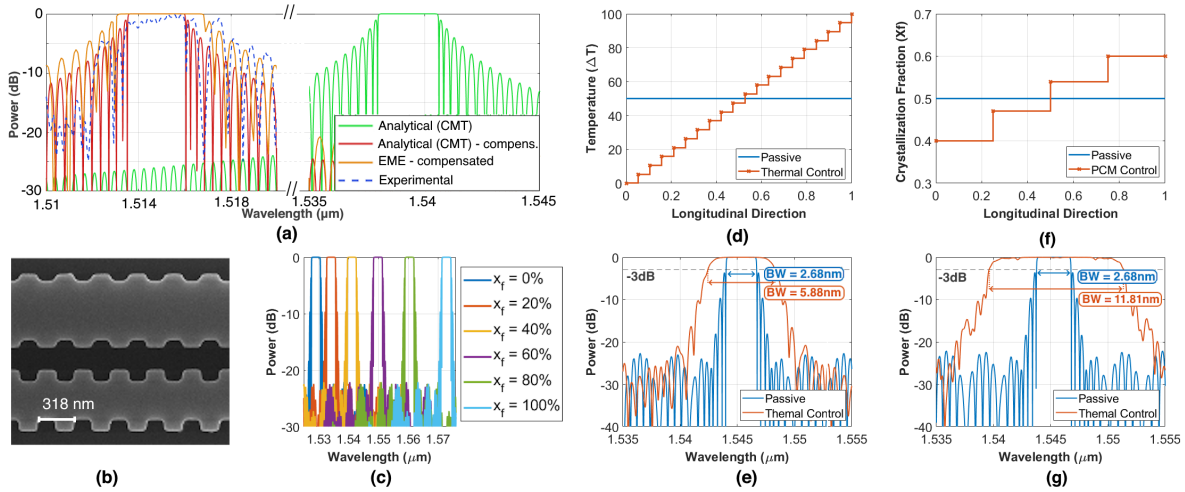

Fig. 2: (a) Response of the fabricated GACDC in comparison to the simulated structure and post-fabrication simulation. (b) SEM image of part of the GACDC fabricated, showing some smoothing in the gratings. (c) Effect of crystallization fraction on the central response of the GACDC. Chirping profiles and bandwidth tunability ranges for (d,e) thermal control of the silicon waveguide and (f,g) proposed control of the PCM layer crystallization fraction.

and smoothing of the grating profile[18] (see Figs. 2(a) and 2(b)). These effects are accounted for in the fitted model by simulating the as-fabricated geometry using EME, and adjusting the waveguide effective index curves and coupling coefficients in the CMT model. Due to its greater flexibility, the CMT model was used for subsequent simulations. The parameters were calibrated through the geometric simulations on the Lumerical platform. The contra-directional coupling coefficient κ=14 × 10^3 was determined to offer the best fit with respect to the experimental results, showing a bandwidth of BW=2.68 nm.

Following model validation, we simulated the device response by varying X_f, as depicted in Fig. 2(c): applying different X_f biases allows sweep of the channel along the entire C-band. To dynamically control the drop-response bandwidth of the GACDC, chirping techniques are necessary. Modulating the effective indices along the propagation direction creates multiple regions with different phase-match conditions, enabling the shaping of the drop spectrum, since the device response is equivalent to the cascaded response of these regions. The conventional bandwidth control consists of introducing a monotone thermal gradient across the device, with respect to the room temperature (ΔT) . This method, shown in Fig. 2(d,e), leads to a bandwidth tunability range of ΔBW=3.2 nm for the maximum thermal range of ΔT=100 ℃, representing a reasonable temperature range. The passive bandwidth (ΔT=0 ℃) of the device is not considered at room temperature, but instead at ΔT=50 ℃: without any thermal bias the bandwidth adjustment would lead to a shift of the central wavelength, while a positive bias allows for symmetric adjustment, maintaining a consistent central channel[19].

The result of our proposed Sb_2Se_3-based GACDC is presented in Fig. 2(g). The GACDC gratings are covered by PCM and divided into four regions, each of which is controlled by an independent heater. The CMT simulations assume this staircase profile, as shown in Fig. 2(f), while crosstalk between the crystallization states would not compromise the response, with just minor effects on the ripples and the roll-off. Four 147 µm-long heaters based on Ti/TiN with a thickness of 110 nm and a width of 2 µm, and a 600 nm spacing on top of Sb_2Se_3 are used[20]. Our simulation results show that an electric pulse with power of 100 mW with a pulse duration of 4 µs is required to fully crystallize the PCM. Like in the thermal case, we bias the device to X_f=0.5 to maintain a consistent central wavelength. By introducing a crystallization chirp of 20% along the device, the tunability range of the bandwidth is increased to $\Delta BW \approx$ 9.13 nm. Higher X_f gradients could extend the bandwidth further, but introduce notch in the drop response. Longer devices can mitigate this problem, but the comparison with the thermal tuning scheme would become unfair, as the bottleneck of T-O control is the maximum temperature change instead of the length.

Conclusion

We presented a Sb_2Se_3-enhanced GACDC that offers three times the dynamic bandwidth control compared to thermally controlled GACDCs, while considering the same number of grating periods to ensure flat-top behavior in both schemes. The Sb_2Se_3 control scheme provides a further improvement in bandwidth tunability for longer devices, far beyond the thermal bottleneck of traditional solutions. In addition, the effective index shift, available through the crystallization fraction bias control in Sb_2Se_3, allows for the nonvolatile tuning of the channel across the entire C-band, which is infeasible through thermal-only control techniques.

Acknowledgements

This work was supported in part by the National Science Foundation (NSF) under grant number CNS-2046226.

References

[1] M. Hammood *et al.*, "Broadband, silicon photonic, optical add–drop filters with 3 dB bandwidths up to 11 THz", *Opt. Lett.*, vol. 46, no. 11, pp. 2738–2741, Jun. 2021. DOI: 10.1364/OL.423745. [Online]. Available: https://opg.optica.org/ol/abstract.cfm?URI=ol-46-11-2738.

[2] M. T. Boroojerdi *et al.*, "Two-period contra-directional grating assisted coupler", *Opt. Express*, vol. 24, no. 20, pp. 22 865–22 874, Oct. 2016. DOI: 10.1364/OE.24.022865. [Online]. Available: https://opg.optica.org/oe/abstract.cfm?URI=oe-24-20-22865.

[3] H. Qiu *et al.*, "Silicon mode multi/demultiplexer based on multimode grating-assisted couplers", *Opt. Express*, vol. 21, no. 15, pp. 17 904–17 911, Jul. 2013. DOI: 10.1364/OE.21.017904. [Online]. Available: https://opg.optica.org/oe/abstract.cfm?URI=oe-21-15-17904.

[4] Z. Xu *et al.*, "Compact silicon-based tm-pass/te-divide polarization beam splitter using contra-directional grating couplers assisted by horizontal slot waveguide", *Optics Communications*, vol. 451, pp. 17–22, 2019, ISSN: 0030-4018. DOI: https://doi.org/10.1016/j.optcom.2019.05.054. [Online]. Available: https://www.sciencedirect.com/science/article/pii/S0030401819304778.

[5] H. Qiu *et al.*, "Narrow-band add-drop filter based on phase-modulated grating-assisted contra-directional couplers", *J. Lightwave Technol.*, vol. 36, no. 17, pp. 3760–3764, Sep. 2018. [Online]. Available: https://opg.optica.org/jlt/abstract.cfm?URI=jlt-36-17-3760.

[6] J. Cauchon *et al.*, "Thermally chirped contra-directional couplers for residueless, bandwidth-tunable bragg filters with fabrication error compensation", *Opt. Lett.*, vol. 46, no. 3, pp. 532–535, Feb. 2021. DOI: 10.1364/OL.413142. [Online]. Available: https://opg.optica.org/ol/abstract.cfm?URI=ol-46-3-532.

[7] A. Shafiee, S. Pasricha, and M. Nikdast, "A survey on optical phase-change memory: The promise and challenges", *IEEE Access*, vol. 11, pp. 11 781–11 803, 2023.

[8] W. Shi, X. Wang, C. Lin, *et al.*, "Silicon photonic grating-assisted, contra-directional couplers", *Optics express*, vol. 21, no. 3, pp. 3633–3650, 2013.

[9] W. Shi *et al.*, "Single-band add-drop filters using anti-reflection, contra-directional couplers", in *The 9th International Conference on Group IV Photonics (GFP)*, 2012, pp. 21–23. DOI: 10.1109/GROUP4.2012.6324073.

[10] L. Tunesi, M. A. Mahdian, A. Carena, V. Curri, M. Nikdast, and P. Bardella, "Segmented design and control in contra-directional coupler for large bandwidth tunability", in *Optical Components and Materials XXI*, SPIE, vol. 12882, 2024, pp. 52–57.

[11] M. A. Mahdian *et al.*, "Bandwidth-adaptive single- and double-channel silicon photonic contra-directional couplers", in *IPC*, 2023.

[12] C. Ríos, M. Stegmaier, P. Hosseini, *et al.*, "Integrated all-photonic non-volatile multi-level memory", *Nature Photonics*, vol. 9, no. 11, pp. 725–732, Nov. 2015, ISSN: 1749-4893. DOI: 10.1038/nphoton.2015.182. [Online]. Available: https://doi.org/10.1038/nphoton.2015.182.

[13] K. Aryana *et al.*, "Optical and thermal properties of Ge2Sb2Te5, Sb2Se3, and Sb2S3 for reconfigurable photonic devices", *Opt. Mater. Express*, vol. 13, no. 11, pp. 3277–3286, Nov. 2023. DOI: 10.1364/OME.503178. [Online]. Available: https://opg.optica.org/ome/abstract.cfm?URI=ome-13-11-3277.

[14] C. Ríos *et al.*, "Ultra-compact nonvolatile phase shifter based on electrically reprogrammable transparent phase change materials", *PhotoniX*, vol. 3, no. 1, p. 26, 2022.

[15] H. Hu *et al.*, "Contra-directional switching enabled by Si-GST grating", *Opt. Express*, vol. 28, no. 2, pp. 1574–1584, Jan. 2020. DOI: 10.1364/OE.381502. [Online]. Available: https://opg.optica.org/oe/abstract.cfm?URI=oe-28-2-1574.

[16] Ansys, *Lumerical FDTD & MODE eigenmode expansion (EME) solvers*, https://optics.ansys.com/hc/en-us/articles/360034396614-MODE-EigenMode-Expansion-EME-solver-introduction, Accessed: [2024].

[17] J.-P. Weber, "Spectral characteristics of coupled-waveguide Bragg-reflection tunable optical filter", English, *IEE Proceedings J (Optoelectronics)*, vol. 140, 275–284(9), 5 Oct. 1993, ISSN: 0267-3932. [Online]. Available: https://digital-library.theiet.org/content/journals/10.1049/ip-j.1993.0045.

[18] S. Lin, M. Hammood, H. Yun, E. Luan, N. A. Jaeger, and L. Chrostowski, "Computational lithography for silicon photonics design", *IEEE Journal of Selected Topics in Quantum Electronics*, vol. 26, no. 2, pp. 1–8, 2019.

[19] L. Tunesi *et al.*, "Thermal control scheme in contra-directional couplers for centered tunable bandwidths", in *NUSOD*, 2023, pp. 115–116. DOI: 10.1109/NUSOD59562.2023.10273529.

[20] A. Shafiee *et al.*, "Design space exploration for PCM-based photonic memory", in *ACM GLSVLSI*, 2023, pp. 533–538.